4020 Organometallics **1996,** *15,* 4020−4029

Solution Thermochemical and Structural Studies of Ligand Substitution of *N*-Pyrrolyl-Substituted Phosphine Ligands in the Cp′Ru(PR$_3$)$_2$Cl (Cp′ = η^5-C$_5$H$_5$ and η^5-C$_5$Me$_5$) Systems

Chunbang Li, Scafford Serron, and Steven P. Nolan*

Department of Chemistry, University of New Orleans, New Orleans, Louisiana 70148

Jeffrey L. Petersen

Department of Chemistry, West Virginia University, Morgantown, West Virginia 26506-6045

Received April 4, 1996[⊗]

The enthalpies of reaction of Cp′Ru(COD)Cl (**1**) (Cp′ = η^5-C$_5$H$_5$ and η^5-C$_5$Me$_5$; COD = cyclooctadiene) with a series of N-pyrrolyl-substituted monodentate tertiary phosphine ligands, leading to the formation of Cp′Ru(PR$_3$)$_2$Cl (PR$_3$ = P(NC$_4$H$_4$)$_3$; P(NC$_4$H$_4$)$_2$(C$_6$H$_5$), P(NC$_4$H$_4$)(C$_6$H$_5$)$_2$, P(NC$_4$H$_8$)$_3$), have been measured by anaerobic solution calorimetry in THF at 30.0 °C. These reactions are rapid and quantitative. Structural studies have been carried out on five complexes in this series, and a discussion of bond length−bond strength relationships is presented. The measured reaction enthalpies span a range of 5 kcal/mol. This series of ligands include some of the most weakly bound phosphines calorimetrically investigated within these two related organometallic systems. Relative importance of phosphine steric vs electronic ligand parameters is more closely examined in terms of the presented quantitative thermochemical and structural information. Comparisons with enthalpy data in related organometallic systems are also presented.

Introduction

A class of ligands which researchers have attempted to characterize in terms of relative importance of ligand steric and electronic effects[1−3] is tertiary phosphines. Such ligands have shown great utility in organometallic chemistry and catalysis as a way to fine tune metal reactivity and selectivity.[4−6] We have been interested in clarifying the exact partitioning of steric and electronic ligand contributions present in tertiary phosphine-based systems.[7,8] We have achieved this in part for one iron- and two ruthenium-based organometallic systems using solution calorimetric techniques.

$$\mathrm{Cp^*Ru(COD)Cl(soln) + 2PR_3(soln) \xrightarrow[30\ ^\circ C]{THF} Cp^*Ru(PR_3)_2Cl(soln) + COD(soln)} \quad (1)$$

$$\mathrm{CpRu(COD)Cl(soln) + 2PR_3(soln) \xrightarrow[30\ ^\circ C]{THF} CpRu(PR_3)_2Cl(soln) + COD(soln)} \quad (2)$$

$$\mathrm{(BDA)Fe(CO)_3(soln) + 2PR_3(soln) \xrightarrow[50\ ^\circ C]{THF}} \textit{trans}\mathrm{-(PR_3)_2Fe(CO)_3(soln) + BDA(soln)} \quad (3)$$

Cp = C$_5$H$_5$; Cp* = C$_5$Me$_5$;
BDA = PhCH═CHCOMe; PR$_3$ = tertiary phosphine

Thermochemical studies performed on organometallic systems have gained recognition as an area of research

---

[⊗] Abstract published in *Advance ACS Abstracts,* August 15, 1996.

(1) (a) Rahman, M. M.; Liu, H.-Y.; Eriks, K.; Prock, A.; Giering, W. P. *Organometallics* **1989**, *8*, 1−7. (b) Liu, H.-Y.; Eriks, K.; Prock, A.; Giering, W. P. *Inorg. Chem.* **1989**, *28*, 1759−1763. (c) Poë, A. J. *Pure Appl. Chem.* **1988**, *60*, 1209−1216 and references cited. (d) Gao, Y.-C; Shi, Q.-Z; Kersher, D. L.; Basolo, F. *Inorg. Chem.* **1988**, *27*, 188−191. (e) Baker, R. T.; Calabrese, J. C.; Krusic, P. J.; Therien, M. J.; Trogler, W. C. *J. Am. Chem. Soc.* **1988**, *110*, 8392−8412. (f) Rahman, M. M.; Liu, H.-Y.; Prock, A.; Giering, W. P. *Organometallics* **1987**, *6*, 650−658.

(2) (a) Huynh, M. H. V.; Bessel, C. A.; Takeuchi, K. J. Presented at the 208th American Chemical Society Meeting; Abstract INOR 165. (b) Perez, W. J.; Bessel, C. A.; See, R. F.; Lake, C. H.; Churchill, M. R.; Takeuchi, K. J. Presented at the 208th American Chemical Society Meeting; Abstract INOR 166. (c) Ching, S.; Shriver, D. F. *J. Am. Chem. Soc.* **1989**, *111*, 3238−3243. (d)Lee, K.-W.; Brown, T. L. *Inorg. Chem.* **1987**, *26*, 1852−1856. (e) Brown, T. L.; Lee, K. J. *Coord. Chem. Rev.* **1993**, *128*, 89−116.

(3) Lorsbach, B. A.; Prock, A.; Giering, W. P. *Organometallics* **1995**, *14*, 1694−1699 and references cited.

(4) (a) Collman, J. P.; Hegedus, L. S.; Norton, J. R.; Finke, R. G. *Principles and Applications of Organotransition Metal Chemistry,* 2nd ed.; University Science: Mill Valley, CA, 1987. (b) Bennett, M. A.; Matheson, T. W. In *Comprehensive Organometallic Chemistry*; Wilkinson, G., Stone, F. G. A., Abel, E. W., Eds.; Pergamon Press: Oxford, England; Chapter 32.9.

(5) (a)Tolman, C. A. *Chem. Rev.* **1977**, *77*, 313−348. (b) Pignolet, L. H., Ed. *Homogeneous Catalysis with Metal Phosphine Complexes*; Plenum: New York, 1983.

(6) Noyori, R. *Asymmetric Catalysis in Organic Synthesis*; Wiley and Sons, Inc.: New York, 1994, and references cited therein.

(7) For organoruthenium systems see: (a) Nolan, S. P.; Martin, K. L.; Stevens, E. D.; Fagan, P. J. *Organometallics* **1992**, *11*, 3947−3953. (b) Luo, L.; Fagan, P. J.; Nolan, S. P. *Organometallics* **1993**, *12*, 4305−4311. (c) Luo, L.; Zhu, N.; Zhu, N.-J.; Stevens, E. D.; Nolan, S. P.; Fagan, P. J. *Organometallics* **1994**, *13*, 669−675. (d) Li, C.; Cucullu, M. E.; McIntyre, R. A.; Stevens, E. D.; Nolan, S. P. *Organometallics* **1994**, *13*, 3621−3627. (e) Luo, L.; Nolan, S. P. *Organometallics* **1994**, *13*, 4781−4786. (f) Cucullu, M. E.; Luo, L.; Nolan, S. P.; Fagan, P. J.; Jones, N. L.; Calabrese, J. C. *Organometallics* **1995**, *14*, 289−296. (g) Luo, L.; Li, C.; Cucullu, M. E.; Nolan, S. P. *Organometallics* **1995**, *14*, 1333−1338. (h) Serron, S. A.; Nolan, S. P. *Organometallics* **1995**, *14*, 4611−4616. (i) Serron, S. A.; Luo, L.; Li, C.; Cucullu, M. E.; Nolan, S. P. *Organometallics* **1995**, *14*, 5290−5297.

(8) For organoiron system see: (a) Luo, L.; Nolan, S. P. *Organometallics* **1992**, *11*, 3483−3486. (b) Luo, L.; Nolan, S. P. *Inorg. Chem.* **1993**, *32*, 2410−2415. (c) Li, C.; Nolan, S. P. *Organometallics* **1995**, *14*, 1327−1332. (d) Li, C.; Stevens, E. D.; Nolan, S. P. *Organometallics* **1995**, *14*, 3791−3797.

S0276-7333(96)00265-8 CCC: $12.00

that can provide important insights into reactivity and bonding patterns.[9−12] In our continuing efforts to map out the thermodynamic parameters associated with this important ligand class, the newly synthesized class of *N*-pyrrolyl tertiary phosphine compounds reported by Moloy and Petersen is of particular interest.[13] Moloy[13] has shown these ligands to undergo quantitative binding to the RhCl(CO) fragment:

$$[\mathrm{RhCl(CO)_2}]_2 + 4\mathrm{PR_3} \rightarrow 2\mathrm{RhCl(CO)(PR_3)_2} + 2\mathrm{CO} \qquad (4)$$

$$\mathrm{PR_3} = \mathrm{P(NC_4H_4)_3};\ \mathrm{P(NC_4H_4)_2Ph};\ \mathrm{P(NC_4H_4)Ph_2};\ \mathrm{P(NC_4H_8)_3}$$

The pyrrolyl moiety, known for its π-involvement (back-donation from metal to ligand) should greatly affect the binding ability of the phosphine. This has been qualitatively demonstrated by infrared spectroscopy in the rhodium system.

The present contribution focuses on quantitatively addressing the binding ability of a series of *N*-pyrrolyl-substituted phosphine ligands in two related organoruthenium systems. Furthermore, structural investigations were carried out on five complexes in the present series and allow for a wider sampling and examination of bond length variation with change in ancillary ligation. A combination of enthalpy and structural data also allows for a discussion of π effects/involvement in the present systems.

Experimental Section

General Considerations. All manipulations involving organoruthenium complexes were performed under inert atmospheres of argon or nitrogen using standard high-vacuum or Schlenk tube techniques or in a Vacuum/Atmospheres glovebox containing less than 1 ppm oxygen and water. Ligands were synthesized according to reported literature procedures.[13] Solvents were dried and distilled under dinitrogen before use by employing standard drying agents.[14] Only materials of high purity as indicated by IR and NMR spectroscopies were used in the calorimetric experiments. NMR spectra were recorded using a Varian Gemini 300 MHz spectrometer. Calorimetric measurements were performed using a Calvet calorimeter (Setaram C-80) which was periodically calibrated using the TRIS reaction[15] or the enthalpy of solution of KCl in water.[16] The experimental enthalpies for these two standard reactions compared very closely to literature values. This calorimeter has been previously described,[17] and typical procedures are described below. Experimental enthalpy data are reported with 95% confidence limits. Elemental analyses were performed by Oneida Research Services, Whitesboro, NY.

Synthesis. The compounds CpRu(COD)Cl,[18] $(\mathrm{Cp^*RuCl})_4$,[19] and Cp*Ru(COD)Cl[19] were synthesized according to literature procedures. Experimental synthetic procedures, leading to isolation of crystalline materials, for previously unreported complexes are described below.

$\mathrm{Cp^*Ru(P(NC_4H_4)_3)_2Cl}$ (2). A 50 mL flask of a high-vacuum frit assembly was charged with 100 mg (0.263 mmol) of Cp*Ru(COD)Cl, 121 mg (0.526 mmol) of $\mathrm{P(NC_4H_4)_3}$, and 20 mL of dried THF. After being stirred overnight, the solution was placed under vacuum to remove volatiles. The residue was then dissolved in 10 mL of THF, the solution was filtered, and 20 mL of pentane was vacuum transferred and layered above the THF solution. Slow cooling of this solution afforded microcrystalline solid which was filtered off and washed with pentane affording 107 mg of the desired product (56% yield). ^{1}H-NMR (300 MHz, THF-d_8): 1.37 (s, 15H, Cp*), 6.07 (s, 12H, pyrrole), 6.55 (s, 12H, pyrrole). Calcd for $\mathrm{C_{34}H_{39}ClN_6P_2Ru}$: C, 55.93; H, 5.34; N, 11.51. Found: C, 56.01; H, 5.29; N, 11.26.

$\mathrm{Cp^*Ru(P(NC_4H_4)_2(C_6H_5))_2Cl}$ (3). A 50 mL flask of a high-vacuum frit assembly was charged with 100 mg (0.263 mmol) of Cp*Ru(COD)Cl, 127.1 mg (0.529 mmol) of $\mathrm{PPh(NC_4H_4)_2}$, and 20 mL of THF. The red orange solution was stirred overnight. This solution was filtered, and the filtrate was evacuated to dryness. The residue was dried thoroughly for 4 h under high vacuum. The residue was dissolved in 15 mL of THF and filtered, and the volume was reduced to 7 mL. A 35 mL volume of pentane was layered above the THF solution and allowed to diffuse overnight, during which time orange needle shaped crystals grew. Cold filtration and washing the crystals with 5 mL of pentane afforded 198 mg of the product (50% yield). ^{1}H-NMR (300 MHz, THF-d_8): 1.25 (s, 15H, Cp*), 5.82 (s, 4H, pyrrole), 6.15 (s, 4H, pyrrole), 6.79 (s, 8H, pyrrole), 7.12−7.26 (m, 10H, Ph). Calcd for $\mathrm{C_{38}H_{41}ClN_4P_2Ru}$: C, 60.67; H, 5.45; N, 7.45. Found: C, 60.47; H, 5.42; N, 7.35.

$\mathrm{Cp^*Ru(P(C_6H_5)_2(NC_4H_4))_2Cl}$ (4). A 50 mL flask of a high-vacuum frit assembly was charged with 103 mg (0.092 mmol) of $(\mathrm{Cp^*RuCl})_4$, 185 mg (7.36 mmol) of $\mathrm{PPh_2(NC_4H_4)}$, and 25 mL of THF. The red solution was stirred overnight. After removal of volatiles under reduced pressure, the residue was dissolved in 15 mL of THF and layered with 30 mL of pentane. Slow diffusion yielded red orange crystals. Yield: 122 mg (42% yield). ^{1}H-NMR (300 MHz, THF-d_8): 1.10, (s, 15H, Cp*), 6.06, (s, 4H, pyrrole), 6.75, (s, 4H, pyrrole), 7.02−7.55, (m, 20H, Ph). Calcd for $\mathrm{C_{42}H_{43}ClN_2P_2Ru}$: C, 65.15; H, 5.60; N, 3.62. Found: C, 65.28; H, 5.64; N, 3.54.

$\mathrm{Cp^*Ru(P(NC_4H_8)_3)_2Cl}$ (5). A 100 mL flask of a high-vacuum frit assembly was charged with 300 mg (0.275 mmol) of $(\mathrm{Cp^*RuCl})_4$, 543 mg (3.201 mmol) of $\mathrm{P(NC_4H_8)_3}$, and 40 mL of THF. The dark blue solution was stirred overnight. This solution was filtered, and the filtrate was evacuated to dryness to yield a orange colored solid. The residue was dried

---

[9] For leading references in this area see: (a) Nolan, S. P. Bonding Energetics of Organometallic Compounds. In *Encyclopedia of Inorganic Chemistry*; J. Wiley and Sons: New York, 1994. (b) Hoff, C. D. *Prog. Inorg. Chem.* **1992**, *40*, 503−561. (c) Martinho Simões, J. A.; Beauchamp, J. L. *Chem. Rev.* **1990**, *90*, 629−688. (d) Marks, T. J. Ed. *Bonding Energetics In Organometallic Compounds*; ACS Symposium Series; American Chemical Society: Washington, DC, 1990; Vol. 428. (e) Marks, T. J., Ed. Metal-Ligand Bonding Energetics in Organotransition Metal Compounds. *Polyhedron Symposium-in-Print*; Elsevier: Amsterdam, 1977; Vol. 7.

[10] See for example: (a) Nolan, S. P.; Hoff, C. D.; Stoutland, P. O.; Newman, L. J.; Buchanan, J. M.; Bergman, R. G.; Yang, G. K.; Peters, K. G. *J. Am. Chem. Soc.* **1987**, *109*, 3143−3145 and references therein. (b) Nolan, S. P.; Lopez de la Vega, R.; Hoff, C. D. *Organometallics* **1986**, *5*, 2529−2537.

[11] (a) Nolan, S. P.; Porchia, M. Marks, T. J. *Organometallics* **1991**, *10*, 1450−1457. (b) Nolan, S. P.; Stern, D.; Marks, T. J. *J. Am Chem. Soc.* **1989**, *111*, 7844−7854.

[12] (a) Nolan, S. P.; Stern, D.; Hedden, D.; Marks, T. J. In ref 1d, pp 159−174. (b) Nolan, S. P.; Lopez de la Vega, R.; Mukerjee, S. L.; Gongalez, A. A.; Hoff, C. D. In ref 1e, pp 1491−1498. (c) Marks, T. J.; Gagné, M. R.; Nolan, S. P.; Schock, L. E.; Seyam, A. M.; Stern, D. L. *Pure Appl. Chem.* **1989**, *61*, 1665−1672. (d) Schock, L. E.; Marks, T. J. *J. Am Chem. Soc.* **1988**, *110*, 7701−7715.

[13] Moloy, K. G.; Petersen, J. L. *J. Am. Chem. Soc.* **1995**, *117*, 7696−7710.

[14] Perrin, D. D.; Armarego, W. L. F. *Purification of Laboratory Chemicals*, 3rd ed.; Pergamon Press: New York, 1988.

[15] Ojelund, G.; Wadsö, I. *Acta Chem. Scand.* **1968**, *22*, 1691−1699.

[16] Kilday, M. V. *J. Res. Natl. Bur. Stand. (U.S.)* **1980**, *85*, 467−481.

[17] (a) Nolan, S. P.; Hoff, C. D.; Landrum, J. T. *J. Organomet. Chem.* **1985**, *282*, 357−362. (b) Nolan, S. P.; Lopez de la Vega, R.; Hoff, C. D. *Inorg. Chem.* **1986**, *25*, 4446−4448.

[18] Albers, M. O.; Robinson, D. J.; Shaver, A.; Singleton, E. *Organometallics* **1986**, *5*, 2199−2205.

[19] (a) Fagan, P. J.; Ward, M. D.; Caspar, J. V.; Calabrese, J. C.; Krusic, P. J. *J. Am. Chem. Soc.* **1988**, *110*, 2981−2983. (b) Fagan, P. J.; Ward, M. D.; Calabrese, J. C. *J. Am. Chem. Soc.* **1989**, *111*, 1698−1719, and references therein. (c) Fagan, P. J.; Mahoney, W. S.; Calabrese, J. C.; Williams, I. D. *Organometallics* **1990**, *9*, 1843−1852.

Table 1. Enthalpies of Substitution (kcal/mol) in the Reaction

$$\mathrm{Cp^*Ru(COD)Cl(soln)} + \mathrm{2L(soln)} \xrightarrow[30\ ^\circ\mathrm{C}]{\mathrm{THF}} \mathrm{Cp^*Ru(L)_2Cl(soln)} + \mathrm{COD(soln)}$$

L	complex	$-\Delta H_{rxn}$[a]
$AsEt_3$	$Cp^*Ru(AsEt_3)_2Cl$	15.0(0.2)[b]
PPh_3	$Cp^*Ru(PPh_3)_2Cl$	18.1(0.2)[b]
$P(p\text{-}CF_3C_6H_4)_3$	$Cp^*Ru(P(p\text{-}CF_3C_6H_4)_3)_2Cl$	20.7(0.2)[c]
$P(NC_4H_4)Ph_2$	$Cp^*Ru[P(NC_4H_4)Ph_2]_2Cl$	20.7(0.4)[d]
$P(NC_4H_4)_3$	$Cp^*Ru[P(NC_4H_4)_3]_2Cl$	21.5(0.4)[d]
$P(p\text{-}ClC_6H_4)_3$	$Cp^*Ru(P(p\text{-}ClC_6H_4)_3)_2Cl$	21.7(0.4)[c]
$P(p\text{-}CH_3OC_6H_4)_3$	$Cp^*Ru(P(p\text{-}CH_3OC_6H_4)_3)_2Cl$	21.8(0.4)[c]
$P(p\text{-}FC_6H_4)_3$	$Cp^*Ru(P(p\text{-}FC_6H_4)_3)_2Cl$	22.0(0.5)[c]
$P(NC_4H_4)_2Ph$	$Cp^*Ru[P(NC_4H_4)_2Ph]_2Cl$	22.1(0.4)[d]
$P(NC_4H_8)_3$	$Cp^*Ru[P(NC_4H_8)_3]_2Cl$	23.8(0.4)[d]
P^nBu_3	$Cp^*Ru(P^nBu_3)_2Cl$	26.0(0.2)[b]
PEt_3	$Cp^*Ru(PEt_3)_2Cl$	27.2(0.2)[b]
PPh_2Me	$Cp^*Ru(PPH_2Me)_2Cl$	29.4(0.2)[b]
$P(OPh)_3$	$Cp^*Ru(P(OPh)_3)_2Cl$	31.2(0.2)[b]
$PPhMe_2$	$Cp^*Ru(PPhMe_2)_2Cl$	31.8(0.3)[b]
PMe_3	$Cp^*Ru(PMe_3)_2Cl$	32.2(0.4)[b]
$P(OMe)_3$	$Cp^*Ru(P(OMe)_3)_2Cl$	37.5(0.4)[b]

[a] Enthalpy values are reported with 95% confidence limits. [b] Taken from ref 7b. [c] Taken from ref 7i. [d] This work.

Table 2. Enthalpies of Substitution (kcal/mol) in the Reaction

$$\mathrm{CpRu(COD)Cl(soln)} + \mathrm{2L(soln)} \xrightarrow[30\ ^\circ\mathrm{C}]{\mathrm{THF}} \mathrm{CpRu(L)_2Cl(soln)} + \mathrm{COD(soln)}$$

L	complex	$-\Delta H_{rxn}$[a]
$AsEt_3$	$CpRu(AsEt_3)_2Cl$	19.4(0.2)[b]
PPh_3	$CpRu(PPh_3)_2Cl$	22.9(0.4)[b]
$P(p\text{-}CH_3C_6H_4)_3$	$CpRu(P(p\text{-}CH_3C_6H_4)_3)_2Cl$	23.7(0.3)[c]
$P(p\text{-}ClC_6H_4)_3$	$CpRu(P(p\text{-}ClC_6H_4)_3)_2Cl$	24.0(0.2)[c]
$P(p\text{-}FC_6H_4)_3$	$CpRu(P(p\text{-}FC_6H_4)_3)_2Cl$	24.2(0.2)[c]
$P(p\text{-}CF_3C_6H_4)_3$	$CpRu(P(p\text{-}CF_3C_6H_4)_3)_2Cl$	24.4(0.2)[c]
$P(p\text{-}CH_3OC_6H_4)_3$	$CpRu(P(p\text{-}CH_3OC_6H_4)_3)_2Cl$	24.6(0.3)[c]
$P(NC_4H_4)_2Ph$	$CpRu[P(NC_4H_4)_2Ph]_2Cl$	25.3(0.1)[d]
$P(NC_4H_4)_3$	$CpRu[P(NC_4H_4)_3]_2Cl$	25.8(0.3)[d]
$P(NC_4H_4)Ph_2$	$CpRu[P(NC_4H_4)Ph_2]_2Cl$	26.2(0.3)[d]
$P(NC_4H_8)_3$	$CpRu[P(NC_4H_8)_3]_2Cl$	27.2(0.3)[d]
PPh_2Me	$CpRu(PPh_2Me)_2Cl$	32.8(0.2)[b]
$P(OPh)_3$	$CpRu(P(OPh)_3)_2Cl$	34.1(0.4)[b]
PEt_3	$CpRu(PEt_3)_2Cl$	34.5(0.2)[b]
P^nBu_3	$CpRu(P^nBu_3)_2Cl$	35.4(0.2)[b]
$PPhMe_2$	$CpRu(PPhMe_2)_2Cl$	35.9(0.2)[b]
PMe_3	$CpRu(PMe_3)_2Cl$	38.4(0.4)[b]
$P(OMe)_3$	$CpRu(P(OMe)_3)_2Cl$	41.8(0.2)[b]

[a] Enthalpy values are reported with 95% confidence limits. [b] Taken from ref 7f. [c] Taken from ref 7i. [d] This work.

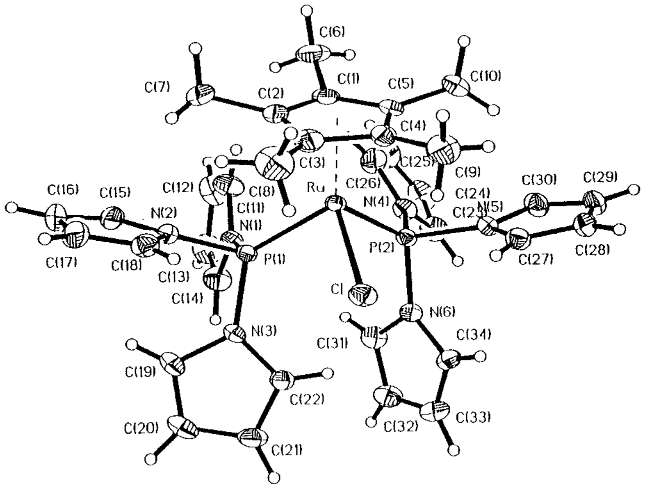

Figure 1. ORTEP of $Cp^*Ru(P(NC_4H_4)_3)_2Cl$ (**2**) with ellipsoids drawn in at 30% probability.

thoroughly for 4 h under high vacuum. It was then dissolved in 35 mL of diethyl ether, filtered, and slowly cooled to −20 °C when red brown crystals was formed. The crystals were cold filtered off and dried under vacuum. Yield: 270 mg (36%). ^{1}H-NMR (300 MHz, C_6D_6): 1.52 (s, 15H, Cp*), 1.59 (m, 16H, pyrrolidinyl), 3.11 (m, 16H, pyrrolidinyl). Calcd for $C_{34}H_{63}ClN_6P_2Ru$: C, 54.09; H, 8.42; N, 11.14. Found: C, 54.66; H, 8.37; N, 11.61.

$Cp^*Ru(P(NC_4H_8)_2Cl)_2Cl$ (6). A 100 mL flask of a high-vacuum frit assembly was charged with 100 mg (0.092 mmol) of $(Cp^*RuCl)_4$, 180 mg of $P(NC_4H_8)_2Cl$, and 25 mL of THF. The pale orange solution was stirred overnight. This solution was filtered, the filtrate was reduced to 2 mL, and 40 mL of pentane was layered above the THF solution. Overnight diffusion afforded orange crystals. Cold filtration followed by a pentane wash afforded 90 mg of the complex (35% yield). ^{1}H-NMR (300 MHz, C_6D_6): 1.58 (s, 15H, Cp*), 3.70−3.20 (s, 24H, pyrrolidinyl), 1.63 (s, 24H, pyrrolidinyl). Calcd for $C_{26}H_{47}Cl_3N_4P_2Ru$: C, 45.58; H, 6.92; N, 8.18. Found: C, 45.45; H, 6.88; N, 7.96.

$CpRu(P(NC_4H_4)_3)_2Cl$ (7). A 150 mg amount of CpRu(COD)Cl and 224 mg of $P(NC_4H_4)_3$ were charged into a round bottom flask of a high-vacuum frit assembly. A 30 mL volume of THF was vacuum transferred, and the pale orange solution was stirred overnight. This solution was filtered, and the filtrate was evacuated to dryness. The residue was dried thoroughly for 4 h under high vacuum. The residue was then dissolved in 10 mL of THF and filtered, and the volume was reduced to 5 mL. The THF solution was then layered with 30 mL of pentane, affording orange crystals after overnight diffusion. Filtration followed by pentane wash afforded 261 mg of the product (82%). ^{1}H-NMR (300 MHz, THF-d_8): 4.96 (s, 5H, Cp), 6.15 (s, 12H, pyrrole), 6.54 (s, 12H, pyrrole). Calcd for $C_{29}H_{29}ClN_6P_2Ru$: C, 52.77; H, 4.43; N, 12.73. Found: C, 53.15; H,4.58; N, 12.61.

$CpRu(P(C_6H_5)(NC_4H_4)_2)_2Cl$ (8). A 178 mg amount of CpRu(COD)Cl and 273 mg of $PPh(NC_4H_4)_2$ were charged into a round bottom flask of a high-vacuum frit assembly. A 30 mL volume of THF was vacuum transferred and the pale orange solution was stirred overnight. This solution was filtered, and the filtrate was evacuated to dryness. The residue was dried thoroughly for 4 h under high vacuum. It was then dissolved in 10 mL of THF. The resulting solution was filtered and the volume reduced to *ca.* 5 mL. A 30 mL volume of pentane was transferred, and the two solvents were allowed to diffuse overnight. Orange crystals were grown in this manner, and upon further slow cooling, the crystals grow larger. Collection of these by cold filtration and drying under vacuum afford the product in a 77% yield (303 mg). ^{1}H-NMR (300 MHz, THF-d_8): 4.70 (s, 5H, Cp), 6.02 (s, 4H, pyrrole), 6.14 (s, 4H, pyrrole), 6.71 (s, 4H, pyrrole), 6.87 (s,4H, pyrrole), 6.95−7.34 (m, 10H, Ph). Calcd for $C_{33}H_{31}ClN_4P_2Ru$: C, 58.11; H, 4.58; N, 8.21. Found: C, 58.20; H, 5.00; N, 8.32.

$CpRu(P(C_6H_5)_2(NC_4H_4))_2Cl$ (9). A 150 mg amount of CpRu(COD)Cl and 244 mg of $PPh_2(NC_4H_4)$ were charged into a round bottom flask of a high-vacuum frit assembly. A 30 mL volume of THF was vacuum transferred, and the pale orange solution was stirred overnight. This solution was filtered, and the filtrate was evacuated to dryness. The residue was dried thoroughly for 4 h under high vacuum. This residue was washed with 10 mL pentane to remove excess phosphine and was dried thoroughly to yield 180 mg of the product (53%). ^{1}H-NMR (300 MHz, THF-d_8): 4.30, (s, 5H, Cp), 6.10, (s, 4H, pyrrole), 6.80, (s, 4H, pyrrole), 7.11−7.37 (m, 20H, Ph). Calcd for $C_{37}H_{33}ClN_2P_2Ru$: C, 63.11; H, 4.72; N, 3.98. Found: C, 63.10; H,4.91; N, 4.18.

$CpRu(P(NC_4H_8)_3)_2Cl$ (10). A 127 mg amount of CpRu(COD)Cl and 204 mg of $P(NC_4H_8)_3$ were charged into a round

Table 3. Summary of Crystallographic Data for 2−4

	(C$_5$Me$_5$)Ru[P(NC$_4$H$_4$)$_3$]$_2$Cl (**2**)	(C$_5$Me$_5$)Ru[P(C$_6$H$_5$)(NC$_4$H$_4$)$_2$]$_2$Cl (**3**)	C$_5$Me$_5$)Ru[P(C$_6$H$_5$)$_2$(NC$_4$H$_4$)]$_2$Cl (**4**)
empirical formula	$C_{34}H_{39}ClN_6P_2Ru$	$C_{38}H_{41}ClN_4P_2Ru$	$C_{42}H_{43}ClN_2P_2Ru$
fw	730.17	752.21	774.24
temp, K	295(2)	295(2)	295(2)
wavelength, Å	0.710 73	0.710 73	0.710 73
cryst system	monoclinic	monoclinic	triclinic
space group	P_21/c	$P2_1/c$	$P\bar{1}$
unit cell dimens			
a, Å	10.964(1)	17.111(2)	11.052(2)
b, Å	16.948(1)	10.233(1)	11.258(2)
c, Å	18.590(2)	20.266(2)	16.311(4)
α, deg	90	90	92.54(2)
β, deg	106.16(1)	101.45(1)	97.41(2)
γ, deg	90	90	114.13(2)
V, Å^3	3317.9(11)	3477.9(11)	1826.1(7)
Z	4	4	2
D(calcd), g/cm^3	1.462	1.437	1.408
abs coeff cm^{-1}	6.84	6.553	6.23
F(100)	1504	1522	800
cryst size, mm	0.28 × 0.36 × 0.50	0.10 × 0.18 × 0.44	0.12 × 0.30 × 0.40
θ range for data collcn, deg	1.93−25.00	2.05−25.00	1.99−25.00
index ranges	$0 \le h \le 12, 0 \le k \le 20, -22 \le l \le 21$	$0 \le h \le 19, 0 \le k \le 12, -24 \le l \le 23$	$0 \le h \le 13, -13 \le k \le 12, -19 \le l \le 19$
no. of collcd reflns	6049	6300	8891
indepdt reflns	5727 ($R_{int} = 0.0207$)	6083 ($R_{int} = 0.0363$)	6410 ($R_{int} = 0.0399$)
refinement method	full-matrix least squares on F^2	full-matrix least squares on F^2	full-matrix least squares on F^2
data/restraints/params	5253/0/402	5417/0/420	5821/0/438
goodness of fig on F^2	1.043	1.022	1.035
final *R* index [$I > 2\sigma(I)$]	$R1 = 0.0413$, w$R2 = 0.0898$	$R1 = 0.0489$, w$R2 = 0.0873$	$R1 = 0.0506$, w$R2 = 0.0994$
R indices (all data)	$R1 = 0.0680$, w$R2 = 0.1025$	$R1 = 0.0974$, w$R2 = 0.1047$	$R1 = 0.0922$, w$R2 = 0.1166$
largest diff peak and hole, e Å^{-3}	0.965 and −0.716	0.614 and −0.316	0.903 and −0.438

bottom flask of a high-vacuum frit assembly. A 30 mL volume of THF was vacuum transferred, and the pale orange solution was stirred overnight. This solution was filtered, and the filtrate was evacuated to dryness. The residue was dried thoroughly for 4 h under high vacuum. The residue was dissolved in 10 mL of THF and filtered, and the volume was reduced to *ca.* 5 mL. A 30 mL volume of pentane was layered above the THF solution, and the two solvents were allowed to diffuse overnight when orange crystals started growing. Slowly cooling the solution to −50 °C afforded larger crystals. These were washed with 5 mL of pentane and dried under vacuum. Yield: 261 mg. (82%). ^{1}H-NMR (300 MHz, C_6D_6): 4.71 (s, 5H, Cp), 3.16−3.31 (d, 24H, pyrrolidinyl), 1.63 (s, 24H, pyrrolidinyl). Calcd for $C_{29}H_{53}ClN_6P_2Ru$: C, 50.91; H, 7.81; N, 12.28. Found: C, 50.69; H, 7.57; N, 12.28.

^{1}H NMR Titrations. Prior to every set of calorimetric experiments involving a new ligand, an accurately weighed amount (±0.1 mg) of the organoruthenium complex was placed in a Wilmad screw-capped NMR tube fitted with a septum, and THF-d_8 was subsequently added. The solution was titrated with a solution of the ligand of interest by injecting the latter in aliquots through the septum with a microsyringe, followed by vigorous shaking. The reactions were monitored by ^{1}H NMR spectroscopy, and the reactions were found to be rapid, clean, and quantitative under experimental calorimetric (temperature and concentration) conditions necessary for accurate and meaningful calorimetric results. These conditions were satisfied for all organoruthenium reactions investigated.

Solution Calorimetry. Calorimetric Measurement of Reaction between Cp*Ru(COD)Cl (1) and P(NC$_4$H$_4$)$_3$. The mixing vessels of the Setaram C-80 were cleaned, dried in an oven maintained at 120 °C, and then taken into the glovebox. A 30−40 mg sample of recrystallized Cp*Ru(COD)Cl was accurately weighed into the lower vessel, which was closed and sealed with 1.5 mL of mercury. A 4 mL volume of a stock solution of P(NC$_4$H$_4$)$_3$ [1 g of P(NC$_4$H$_4$)$_3$ in 25 mL of THF] was added, and the remainder of the cell was assembled, removed from the glovebox, and inserted in the calorimeter. The reference vessel was loaded in an identical fashion with the exception that no organoruthenium complex was added to the lower vessel. After the calorimeter had reached thermal equilibrium at 30.0 °C (about 2 h), the calorimeter was inverted thereby allowing the reactants to mix. After the reaction had reached completion and the calorimeter had once again reached thermal equilibrium (ca. 2 h) the vessels were removed from the calorimeter. Conversion to Cp*Ru(P(NC$_4$H$_4$)$_3$)$_2$Cl was found to be quantitative under these reaction conditions. The enthalpy of reaction, −16.6 ± 0.4 kcal/mol, represents the average of five individual calorimetric determinations. The final enthalpy value listed in Table 1 (−21.5 ± 0.3 kcal/mol) represents the enthalpy of ligand substitution with all species in solution. The enthalpy of solution of **1** (4.9 ± 0.1 kcal/mol) has therefore been subtracted from the −16.6 ± 0.3 kcal/mol value. This methodology represents a typical procedure involving all organometallic compounds and all reactions investigated in the present study.

Structure Determination of Cp*Ru(P(NC$_4$H$_4$)$_3$)$_2$Cl (2). A yellow parallelepiped-shaped crystal of **2**, grown from a 2:5 THF/pentane solution, having approximate dimensions 0.28 × 0.36 × 0.50 mm was sealed in a capillary tube and mounted on the goniostat of a Siemens P4 automated X-ray diffractometer. Data were collected using Mo Kα radiation at 295 K. Cell dimensions were determined by least-squares refinement of the measured setting angles of 40 reflections with $16° < 2\theta < 25°$. The structure was solved using direct methods (SHELXTL PLUS) and refined by full-matrix least-squares techniques. Crystal data for **2** are summarized in Table 3, and selected bond distances and angles are listed in Table 4. Figure 1 gives an ORTEP drawing of this molecule.

Structure Determination of Cp*Ru(P(NC$_4$H$_4$)$_2$(C$_6$H$_5$))$_2$Cl (3). A reddish-orange crystal, grown from slow evaporation of a 1:5 solution of THF/pentane, having approximate dimensions 0.10 × 0.18 × 0.44 mm was placed in a capillary tube and mounted on the goniostat of a Siemens P4 automated X-ray diffractometer. Data were collected using Mo Kα radiation at 295 K. Cell dimensions were determined by least-squares refinement of the measured setting angles of 24 reflections with $20° < 2\theta < 27°$. The structure was solved using direct methods (SHELXTL PLUS) and refined by full-matrix least-squares techniques. Crystal data for **3** are

Table 4. Selected Bond Distances (Å) and Bond Angles (deg) for $(C_5Me_5)Ru[P(NC_4H_4)_3]_2Cl$ (2)

Bond Lengths			
Ru−P (1)	2.2598(11)	Ru−P (2)	2.2639(12)
Ru−Cl	2.4312(12)	Ru−Cp(c)	1.930
P(1)−N(1)	1.712(4)	P(1)−N(2)	1.722(3)
P(1)−N(3)	1.717(3)	P(2)−N(4)	1.712(3)
P(2)−N(5)	1.721(3)	P(2)−N(6)	1.733(3)
N(1)−C(11)	1.386(6)	N(1)−C(14)	1.379(6)
N(2)−C(15)	1.386(5)	N(2)−C(18)	1.378(5)
N(3)−C(19)	1.405(5)	N(3)−C(22)	1.378(5)
N(4)−C(23)	1.391(6)	N(4)−C(26)	1.374(6)
N(5)−C(27)	1.380(5)	N(5)−C(30)	1.388(5)
N(6)−C(31)	1.375(5)	N(6)−C(34)	1.383(5)
Bond Angles			
Cp(c)−Ru−Cl	114.8	Cp(c)−Ru−P(1)	127.0
Cp(c)−Ru−P(2)	126.3	P(1)−Ru−Cl	91.90(5)
P(2)−Ru−Cl	91.05(4)	P(1)−Ru−P(2)	95.83(4)
N(1)−P(1)−N(2)	98.1(2)	N(1)−P(1)−N(3)	100.4(2)
N(2)−P(1)−N(3)	96.0(2)	N(1)−P(1)−Ru	118.20(12)
N(2)−P(1)−Ru	115.83(12)	N(3)−P(1)−Ru	123.45(12)
N(4)−P(2)−N(5)	100.4(2)	N(4)−P(2)−N(6)	95.9(2)
N(5)−P(2)−N(6)	98.6(2)	N(4)−P(2)−Ru	121.56(14)
N(5)−P(2)−Ru	112.65(12)	N(6)−P(2)−Ru	123.22(12)
C(11)−N(1)−C(14)	106.4(4)	C(14)−N(1)−P(1)	131.0(3)
C(11)−N(1)−P(1)	122.4(2)	C(15)−N(2)−C(18)	106.8(4)
C(15)−N(2)−P(1)	129.6(3)	C(18)−N(2)−P(1)	122.4(3)
C(19)−N(3)−C(22)	106.9(3)	C(19)−N(3)−P(1)	124.8(3)
C(22)−N(3)−P(1)	128.2(3)	C(23)−N(4)−C(26)	106.4(4)
C(23)−N(4)−P(2)	129.0(3)	C(26)−N(4)−P(2)	124.7(3)
C(27)−N(5)−C(30)	106.6(4)	C(27)−N(5)−P(2)	123.9(3)
C(30)−N(5)−P(2)	129.5(3)	C(31)−N(6)−C(34)	107.5(3)
C(31)−N(6)−P(2)	125.4(3)	C(34)−N(6)−P(2)	126.8(3)

Table 5. Selected Bond Distances (Å) and Bond Angles (deg) for $(C_5Me_5)Ru[P(C_6H_5)(NC_4H_4)_2]_2Cl$ (3)

Bond Lengths			
Ru−P (1)	2.2871(14)	Ru−P (2)	2.2827(14)
Ru−Cl	2.4373(14)	Ru−Cp(c)	1.911
P(1)−N(1)	1.733(4)	P(1)−N(2)	1.731(4)
P(2)−N(3)	1.719(5)	P(2)−N(4)	1.750(4)
P(1)−C(11)	1.804(5)	P(2)−C(33)	1.836(5)
N(1)−C(17)	1.369(7)	N(1)−C(20)	1.408(6)
N(2)−C(21)	1.400(6)	N(2)−C(24)	1.391(6)
N(3)−C(25)	1.414(7)	N(3)−C(28)	1.366(7)
N(4)−C(29)	1.373(7)	N(4)−C(32)	1.378(7)
Bond Angles			
Cp(c)−Ru−Cl	117.0	Cp(c)−Ru−P(1)	124.8
Cp(c)−Ru−P(2)	127.3	Cl−Ru−P(1)	94.28(5)
P(2)−Ru−Cl	88.18(5)	P(1)−Ru−P(2)	94.54(5)
N(1)−P(1)−Ru	114.0(2)	N(2)−P(1)−Ru	123.6(2)
N(1)−P(1)−N(2)	98.9(2)	C(11)−P(1)−Ru	115.1(2)
N(1)−P(1)−C(11)	102.5(2)	N(2)−P(1)−C(11)	99.5(2)
N(3)−P(2)−Ru	119.3(2)	N(4)−P(2)−Ru	111.9(2)
C(33)−P(2)Ru	124.2(2)	N(3)−P(2)−N(4)	97.9(2)
N(3)−P(2)−C(33)	99.0(2)	N(4)−P(2)−C(33)	100.0(2)
C(17)−N(1)−P(1)	124.3(4)	C(20)−N(1)−P(1)	127.6(4)
C(17)−N(1)−C(20)	106.9(4)	C(21)−N(2)−P(1)	127.1(4)
C(24)−N(2)−P(1)	121.5(3)	C(21)−N(2)−C(24)	108.5(4)
C(25)−N(3)−P(2)	128.8(4)	C(28)−N(3)−P(2)	124.2(4)
C(25)−N(3)−C(28)	106.9(5)	C(29)−N(4)−P(2)	128.9(5)
C(32)−N(4)−P(2)	123.5(4)	C(29)−N(4)−C(32)	107.5(5)

summarized in Table 3, and selected bond distances and angles are listed in Table 5. Figure 2 gives an ORTEP drawing of this molecule.

Structure Determination of $Cp^*Ru(P(NC_4H_4)(C_6H_5)_2)_2Cl$ (4). A reddish-orange crystalline fragment, grown from slow evaporation of a solution of THF/pentane/Et_2O (1:1:3), having approximate dimensions 0.12 × 0.30 × 0.40 mm was mounted in a capillary tube and aligned on the goniostat of a Siemens P4 automated X-ray diffractometer. Data were collected using Mo Kα radiation at 295 K. Cell dimensions were determined by least-squares refinement of the measured setting angles of 24 reflections with 20° < 2θ < 28°. The structure was solved using a combination of Patterson methods and Fourier summations calculated with algorithms provided by SHELXTL IRIS and refined by full-matrix least-squares techniques. Crystal data for **4** are summarized in Table 3, and selected bond distances and angles are listed in Table 6. Figure 3 gives an ORTEP drawing of this molecule.

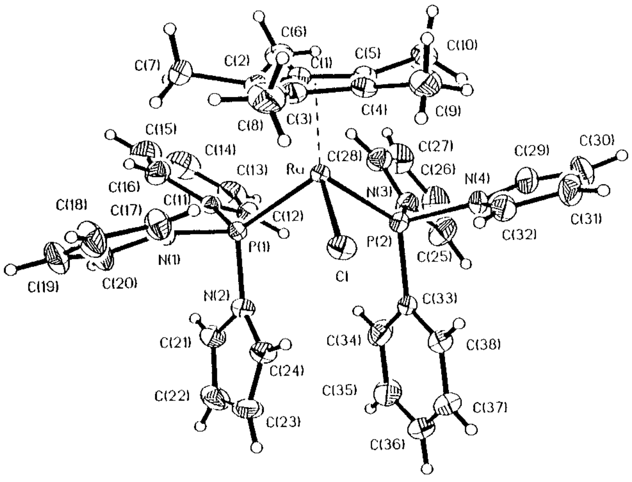

Figure 2. ORTEP of $Cp^*Ru(P(NC_4H_4)_2(C_6H_5))_2Cl$ (**3**) with ellipsoids drawn in at 30% probability.

Table 6. Selected Bond Distances (Å) and Bond Angles (deg) for $(C_5Me_5)Ru[P(C_6H_5)_2(NC_4H_4)]_2Cl$ (4)

Bond Lengths			
Ru−P (1)	2.3064(13)	Ru−P (2)	2.3195(14)
Ru−Cl	2.443(2)	Ru−Cp(c)	1.900
P(1) -N(1)	1.753(5)	P(1)−C(15)	1.821(5)
P(1)−C(21)	1.833(5)	P(2)−N(2)	1.746(4)
P(2)−C(27)	1.821(5)	P(2)−C(37)	1.838(4)
N(1)−C(11)	1.408(6)	N(1)−C(14)	1.379(7)
N(2)−C(33)	1.360(7)	N(2)−C(36)	1.388(6)
Bond Angles			
Cp(c)−Ru−Cl	118.5	Cp(c)−Ru−P(1)	126.5
Cp(c)−Ru−P(2)	125.3	P(1)−Ru−Cl	87.45(6)
P(2)−Ru−Cl	90.30(5)	P(1)−Ru−P(2)	97.87(5)
N(1)−P(1)−C(15)	100.3(2)	N(1)−P(1)−C(21)	98.0(2)
C(15)−P(1)−C(21)	101.0(2)	N(1)−P(1)−Ru	118.8(2)
N(2)−P(2)−C(27)	102.1(2)	N(2)−P(2)−C(37)	95.4(2)
C(27)−P(2)−C(37)	100.7(2)	N(2)−P(2)−Ru	113.4(2)
C(27)−P(2)−Ru	115.1(2)	C(37)−P(2)−Ru	126.14(14)
C(14)−N(1)−C(11)	108.6(5)	C(14)−N(1)−P(1)	124.7(4)
C(11)−N(1)−P(1)	126.7(4)	C(33)−N(2)−C(36)	106.6(5)
C(33)−N(2)−P(2)	126.8(4)	C(36)−N(2)−P(2)	125.6(4)
C(12)−C(11)−N(1)	112.8(6)	N(1)−C(14)−C(13)	109.8(6)
C(16)−C(15)−P(1)	124.8(5)	C(20)−C(15)−P(1)	120.4(4)
C(22)−C(21)−P(1)	122.9(4)	C(26)−C(21)−P(1)	119.6(4)
C(28)−C(27)−P(2)	124.9(4)	C(32)−C(27)−P(2)	117.5(4)
N(2)−C(33)−C(34)	109.0(6)	C(35)−C(36)−N(2)	110.1(5)
C(38)−C(37)−P(2)	117.1(3)	C(42)−C(37)−P(2)	123.9(4)

Structure Determination of $Cp^*Ru(P(NC_4H_8)_3)_2Cl$ (5). A reddish-orange crystalline fragment, grown from slow evaporation of a saturated solution of Et_2O, having approximate dimensions 0.18 × 0.36 × 0.40 mm was sealed in a capillary tube and aligned on the goniostat of a Siemens P4 automated X-ray diffractometer. Data were collected using Mo Kα radiation at 295 K. Cell dimensions were determined by least-squares refinement of the measured setting angles of 30 reflections with 16° < 2θ < 25°. The structure was solved using a combination of Patterson methods and Fourier summations calculated with algorithms provided by SHELXTL IRIS and refined by full-matrix least-squares techniques. Crystal data for **5** are summarized in Table 7, and selected bond distances and angles are listed in Table 8. Figure 4 gives an ORTEP drawing of this molecule.

Structure Determination of $Cp^*Ru(P(NC_4H_8)_2Cl)_2Cl$ (6). A reddish-orange crystal, grown by slow evaporation of a 1:2 THF/pentane solution, having approximate dimensions 0.34 × 0.40 × 0.44 mm was sealed in a capillary tube and aligned on the goniostat of a Siemens P4 automated X-ray

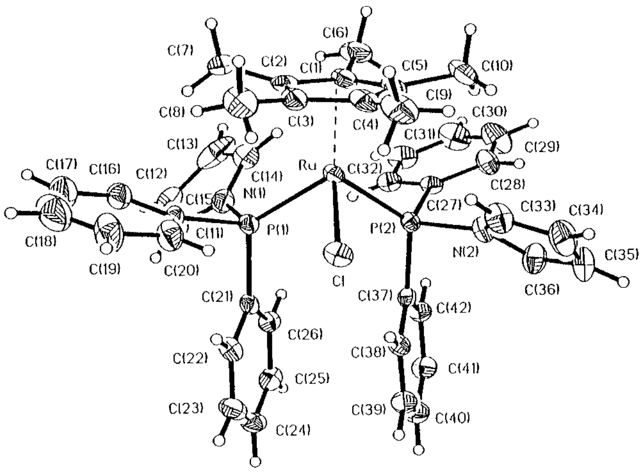

Figure 3. ORTEP of Cp*Ru(P(NC$_4$H$_4$)(C$_6$H$_5$)$_2$)$_2$Cl (**4**) with ellipsoids drawn in at 30% probability.

Table 7. Summary of Crystallographic Data for 5 and 6

	(C$_5$Me$_5$)Ru-[P(NC$_4$H$_8$)$_3$]$_2$Cl (**5**)	(CMe$_5$)Ru-[P(NC$_4$H$_8$)$_2$Cl]$_2$Cl (**6**)
empirical formula	$C_{34}H_{63}ClN_6P_2Ru$	$C_{26}H_{47}Cl_3N_4P_2Ru$
fw	754.36	685.04
temp, K	295(5)	295(2)
space group	$P\bar{1}$	$P2_1/c$
wavelength, Å	0.710 73	0.710 73
cryst system	triclinic	monoclinic
unit cell dimens		
a, Å	11.258(1)	13.217(1)
b, Å	12.223(1)	12.901(1)
c, Å	13.310(1)	18.298(1)
α, deg	85.336(7)	90
β, deg	82.551(9)	94.05(3)
γ, deg	82.784(8)	90
V, Å^3	1797.8(2)	3112.3(5)
Z	2	4
D(calcd), g/cm^3	1.394	1.462
abs coeff, cm^{-1}	6.33	8.9
F(000)	800	1342
cryst size, mm	0.18 × 0.36 × 0.40	0.34 × 0.40 × 0.44
θ range for data collcd, deg	1.84−22.50	1.54−25.00
index ranges	$0 \le h \le 12$, $-13 \le k \le 13$, $-14 \le l \le 14$	$0 \le h \le 15$, $0 \le k \le 15$, $-21 \le l \le 21$
reflcns collcd	4980	5725
indepdt reflcns	4691 ($R_{int} = 0.0229$)	5473 ($R_{int} = 0.0368$)
refinement method	full-matrix least squares on F^2	full-matrix least squares on F^2
data/restraints/params	4430/0/402	4846/0/330
goodness of fit on F^2	1.024	1.020
final *R* indices [$I > 2\sigma(I)$]	$R1 = 0.0386$, $wR2 = 0.0816$	$R1 = 0.0525$, $wR2 = 0.0982$
R indices (all data)	$R1 = 0.0574$, $wR2 = 0.0908$	$R1 = 0.1037$, $wR2 = 0.1167$
largest diff peak and hole, e Å^{-3}	0.350 and −0.286	0.519 and −0.319

diffractometer. Data were collected using Mo Kα radiation at 295 K. Cell dimensions were determined by least-squares refinement of the measured setting angles of 45 reflections with 10° < 2θ < 25°. The structure was solved using direct methods (SHELXTL PLUS) and refined by full-matrix least-squares techniques. Crystal data for **6** are summarized in Table 7, and selected bond distances and angles are listed in Tables 9. Figure 5 gives an ORTEP drawing of this molecule.

Results

A facile entryway into the thermochemistry of Cp′Ru(PR$_3$)$_2$Cl (Cp′ = η^5-C$_5$H$_5$ and η^5-C$_5$Me$_5$) complexes is made possible by the rapid and quantitative reaction of Cp′Ru(COD)Cl (**1**) with the phosphine ligand.[7e−g]

Table 8. Selected Bond Distances (Å) and Bond Angles (deg) for (C$_5$Me$_5$)Ru[P(NC$_4$H$_8$)$_3$]$_2$Cl (5)

Bond Lengths			
Ru−P(1)	2.3477(14)	Ru−P (2)	2.3520(14)
Ru−Cl	2.4534(14)	Ru−Cp(c)	1.943
P(1)−N(1)	1.688(4)	P(1)−N(2)	1.692(4)
P(1)−N(3)	1.695(4)	P(2)−N(4)	1.710(4)
P(2)−N(5)	1.699(4)	P(2)−N(6)	1.698(4)
N(1)−C(11)	1.454(6)	N(1)−C(14)	1.479(6)
N(2)−C(15)	1.478(6)	N(2)−C(18)	1.458(7)
N(3)−C(19)	1.476(6)	N(3)−C(22)	1.466(6)
N(4)−C(23)	1.465(6)	N(4)−C(26)	1.462(6)
N(5)−C(27)	1.470(6)	N(5)−C(30)	1.472(7)
N(6)−C(31)	1.473(6)	N(6)−C(34)	1.474(6)

Bond Angles			
Cp(c)−Ru−Cl	113.7	Cp(c)−Ru−P(1)	126.5
Cp(c)−Ru−P(2)	125.9	P(1)−Ru−Cl	90.84(5)
P(2)−Ru−Cl	92.41(5)	P(1)−Ru−P(2)	97.59(5)
N(1)−P(1)−N(2)	103.6(2)	N(1)−P(1)−N(3)	97.3(2)
N(2)−P(1)−N(3)	100.0(2)	N(1)−P(1)−Ru	117.3(2)
N(2)−P(1)−Ru	110.1(2)	N(3)−P(1)−Ru	125.4(2)
N(4)−P(2)−N(5)	97.6(2)	N(4)−P(2)−N(6)	96.6(2)
N(5)−P(2)−N(6)	105.6(2)	N(4)−P(2)−Ru	120.7(2)
N(5)−P(2)−Ru	110.0(2)	N(6)−P(2)−Ru	122.69(14)
C(11)−N(1)−C(14)	106.8(4)	C(14)−N(1)−P(1)	128.3(3)
C(11)−N(1)−P(1)	124.6(3)	C(15)−N(2)−C(18)	108.8(4)
C(15)−N(2)−P(1)	123.2(4)	C(18)−N(2)−P(1)	124.8(4)
C(19)−N(3)−C(22)	109.9(4)	C(19)−N(3)−P(1)	122.9(3)
C(22)−N(3)−P(1)	125.6(3)	C(23)−N(4)−C(26)	106.9(4)
C(23)−N(4)−P(2)	119.3(3)	C(26)−N(4)−P(2)	118.7(3)
C(27)−N(5)−C(30)	106.7(4)	C(27)−N(5)−P(2)	117.7(3)
C(30)−N(5)−P(2)	127.0(4)	C(31)−N(6)−C(34)	106.2(4)
C(31)−N(6)−P(2)	123.8(3)	C(34)−N(6)−P(2)	119.9(4)

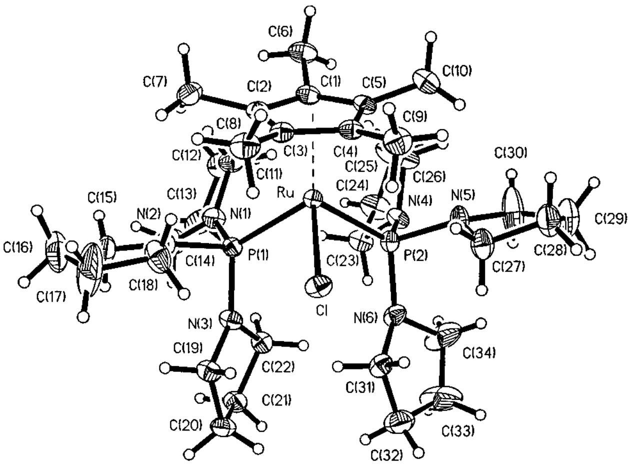

Figure 4. ORTEP of Cp*Ru(P(NC$_4$H$_8$)$_3$)$_2$Cl (**5**) with ellipsoids drawn in at 30% probability.

$$\mathrm{Cp'Ru(COD)Cl(s)} + 2\mathrm{PR_3(soln)} \xrightarrow[30\ ^\circ\mathrm{C}]{\mathrm{THF}} \mathrm{Cp'Ru(PR_3)_2Cl(soln)} + \mathrm{COD(soln)} \quad (5)$$

$$\mathrm{Cp'} = \mathrm{C_5H_5},\ \mathrm{C_5Me_5};\ \mathrm{PR_3} = \text{tertiary phosphine}$$

This type of phosphine binding reaction appears general and was found to be rapid and quantitative for all ligands calorimetrically investigated at 30.0 °C in tetrahydrofuran. A similar use of this entryway has been employed in previous calorimetric studies involving ligand substitution reactions. A compilation of phosphine ligands with their respective enthalpies of reaction, in solution, are presented in Tables 1 and 2.

Single crystal structural studies were carried out on the five new complexes, Cp*Ru(P(NC$_4$H$_4$)$_3$)$_2$Cl (**2**), Cp*Ru-

Table 9. Selected Bond Distances (Å) and Bond Angles (deg) for $(C_5Me_5)Ru[P(NC_4H_8)_2Cl]_2Cl$ (6)

Bond Lengths

Ru−P (1)	2.275(2)	Ru−P (2)	2.265(2)
Ru−Cl(1)	2.433(2)	Ru−Cp(c)	1.905
Cl(2)−P(1)	2.187(2)	Cl(3)−P(2)	2.158(2)
P(1)−N(1)	1.647(5)	P(1)−N(2)	1.661(5)
P(2)−N(3)	1.657(5)	P(2)−N(4)	1.661(5)
N(1)−C(11)	1.471(8)	N(1)−C(14)	1.447(7)
N(2)−C(15)	1.472(8)	N(2)−C(18)	1.464(7)
N(3)−C(19)	1.487(8)	N(3)−C(22)	1.454(7)
N(4)−C(23)	1.452(7)	N(4)−C(26)	1.475(8)

Bond Angles

Cp(c)−Ru−Cl(1)	118.0	Cp(c)−Ru−P(1)	128.5
Cp(c)−Ru−P(2)	124.6	P(1)−Ru−Cl(1)	88.23(6)
P(2)−Ru−Cl(1)	91.12(6)	P(1)−Ru−P(2)	95.63(6)
N(1)−P(1)−N(2)	98.9(3)	N(1)−P(1)−Cl(2)	101.7(2)
N(2)−P(1)−Cl(2)	96.0(2)	N(1)−P(1)−Ru	116.9(2)
N(2)−P(1)−Ru	129.3(2)	Cl(2)−P(1)−Ru	109.34(9)
N(3)−P(2)−N(4)	103.0(3)	N(3)−P(2)−Cl(3)	100.4(2)
N(3)−P(2)−Ru	122.2(2)	N(4)−P(2)−Cl(3)	98.5(2)
N(4)−P(2)−Ru	114.4(2)	Cl(3)−P(2)−Ru	114.92(9)
C(11)−N(1)−P(1)	123.6(5)	C(14)−N(1)−P(1)	127.1(5)
C(11)−N(1)−C(14)	108.1(5)	C(15)−N(2)−P(1)	121.7(4)
C(18)−N(2)−P(1)	126.8(4)	C(15)−N(2)−C(18)	110.3(5)
C(19)−N(3)−P(2)	126.4(5)	C(22)−N(3)−P(2)	123.8(4)
C(19)−N(3)−C(22)	108.2(5)	C(23)−N(4)−P(2)	120.3(4)
C(26)−N(4)−P(2)	126.8(4)	C(23)−N(4)−C(26)	106.8(5)
C(12)−C(11)−N(1)	104.9(6)	N(1)−C(14)−C(13)	105.3(6)
C(20)−C(19)−N(3)	107.7(7)	N(3)−C(22)−C(21)	105.0(5)
N(4)−C(23)−C(24)	103.9(6)	N(4)−C(26)−C(25)	103.6(6)

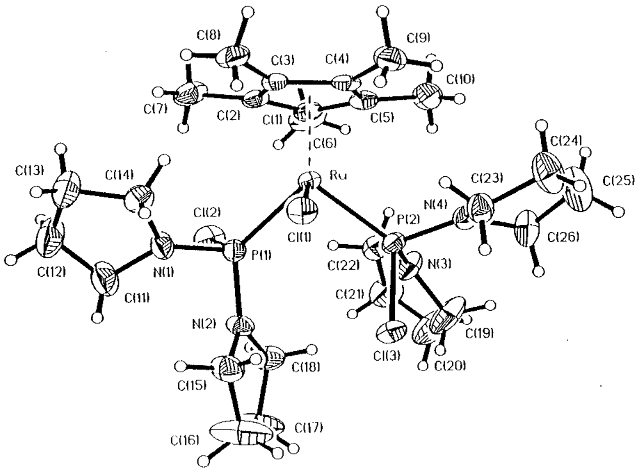

Figure 5. ORTEP of $Cp^*Ru(P(NC_4H_8)_2Cl)_2Cl$ (**6**) with ellipsoids drawn in at 30% probability.

$(P(NC_4H_4)_2(C_6H_5))_2Cl$ (**3**), $Cp^*Ru(P(NC_4H_4)(C_6H_5)_2)_2Cl$ (**4**), $Cp^*Ru(P(NC_4H_8)_3)_2Cl$ (**5**), and $Cp^*Ru(P(NC_4H_8)_2Cl)_2Cl$ (**6**) ($Cp^* = C_5Me_5$).

Discussion

The donor properties of tertiary phosphine ligands can be modulated by electronic and steric parameter variation.[5] This is usually achieved by selective variation of the substituents bound to the phosphorus atom. The binding affinities of specific phosphine ligands are commonly explained in terms of electronic and /or steric effects, yet these two factors are not easily separated. A common approach in physical inorganic/organometallic chemistry is to examine such effects while maintaining one of the two factors constant. The most common approach has been to examine a series of isosteric phosphines.[20] This can be achieved by specific substitution of various para-substituted aryl grouping on a phosphorus center. We have recently reported on the thermochemical effects of such variations in both ruthenium and iron systems.[7i,8c]

$$CpRu(COD)Cl(soln) + 2PR_3(soln) \xrightarrow[30\ °C]{THF} CpRu(PR_3)_2Cl(soln) + COD(soln) \quad (6)$$

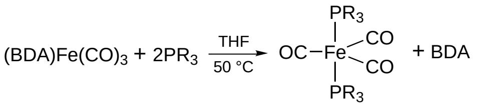

$$(BDA)Fe(CO)_3 + 2PR_3 \xrightarrow[50\ °C]{THF} (PR_3)_2Fe(CO)_3 + BDA \quad (7)$$

$$PR_3 = P(p\text{-}XC_6H_4)_3;\ X = H, Cl, F, Me, MeO, CF_3$$

This approach is however limited, and an expansion of these electronic variations within the isosteric series would prove useful. Furthermore, results of studies invoking the importance of electronic effects oftentimes do not easily distinguish between σ and π contributions.[1]

Moloy and Petersen have reported on the synthesis and binding to rhodium systems of a novel class of *N*-pyrrolyl-substituted tertiary phosphine ligands which are isosteric with triphenylphosphine (and para-substituted triphenylphosphine ligands), with cone angle values of 145⁰ (eq 4).[13] This *N*-pyrrolyl-substituted phosphine series affords a further advantage in that the pyrrolyl provides aromatic delocalization of the nitrogen lone pair into the ring which renders the phosphine ligand less basic. Pertinent resonance structures for the phosphine ligand can be drawn as follows:

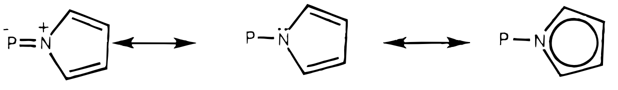

A **B** **C**

In view of the substitution of a more electronegative nitrogen (vs carbon) atom in the ligand, **C** would be expected to be the preferred resonance structure at play if, as is now believed, the pyrolylphosphine acts as a significantly poorer donor than triphenylphosphine.

Solution Thermochemistry. In order to test these qualitative observations, a thermochemical study of ligand substitution reactions involving these novel phosphines was undertaken to quantify these electronic effects. Solution thermochemical studies were performed for two related organoruthenium systems:

$$Cp'Ru(COD)Cl(s) + 2L(soln) \xrightarrow[30\ °C]{THF} Cp'Ru(L)_2Cl(soln) + COD(soln) + \Delta H \quad (8)$$

$$Cp' = C_5H_5, C_5Me_5;\ L = \text{N-substituted phosphines}$$

Enthalpy data are presented in Tables 1 and 2 for the $Cp^*Ru(PR_3)_2Cl$ and $CpRu(PR_3)_2Cl$ systems, respectively. In addition to the N-substituted phosphine ligands, previously investigated phosphines are also presented to afford a numerical comparison. In the Cp system, the new phosphines bind slightly better than the para-substituted phosphines, in the range of −25.3 to −27.2 kcal/mol with the $P(NC_4H_8)_3$ acting as a better donor. For the Cp* system, the N-substituted phosphine ligands are in the −20.7 to −23.8 kcal/mol range

---

[20] A specific example for the two systems discussed here can be found in ref 7i. Other examples can be found in refs 1 and 4a.

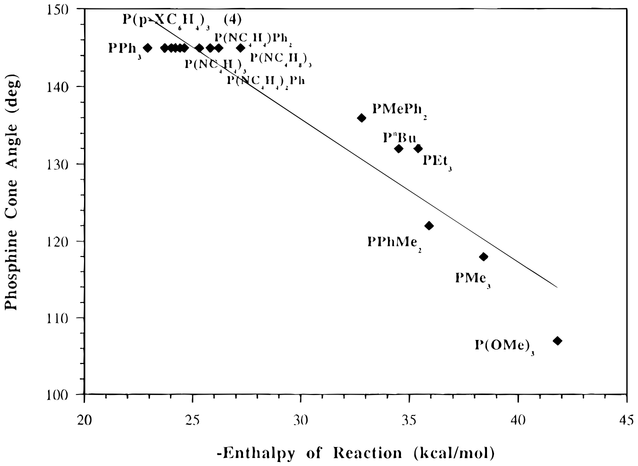

Figure 6. Enthalpies of reaction (kcal/mol) for the CpRu(PR$_3$)$_2$Cl system vs phosphine cone angle (deg). Slope = −1.85; $R = 0.95$

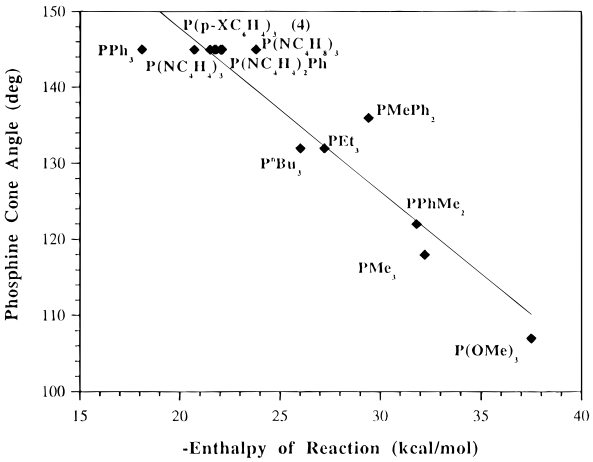

Figure 7. Enthalpies of reaction (kcal/mol) for the Cp*Ru(PR$_3$)$_2$Cl system vs phosphine cone angle (deg). Slope = −2.15; $R = 0.95$.

and are intermingled with the isosteric para-substituted triphenylphosphine series. Here again the pyrrolidinylphosphine is the most exothermic of the series. The loss of aromatic character on going to the pyrrolidinyl substituent eliminates any π back-donation and the phosphine behaves uniquely as a σ donor.[21] However, it is a bit surprising to notice the pyrrolidinyl-substituted phosphine acting as such a poor donor when compared with the rhodium results of Moloy and our recent results on *trans*-(PR$_3$)$_2$Fe(CO)$_3$,[21] where the ligand is comparable to PEt$_3$ on the donor scale. This diminished donor ability is apparently due to steric factors. In both the rhodium and iron systems, the phosphine electronic parameter is the principal contributor to the magnitude of the reaction enthalpy.[21,22] In the ruthenium case, it has been previously shown that sterics dominate.[7e] To test the validity of this point on the present ligand series, such an analysis was carried out and the results are presented in Figures 6 and 7.

The observed correlation is good for all data investigated so far, including the *N*-pyrrolyl- and *N*-pyrrolidinyl-substituted phosphine ligands series.[23] The fact that the new ligand set is isosteric and that steric factors dictate the magnitude of the enthalpies of reaction in the present ruthenium system accounts for the relatively weaker than expected donor ability of the P(NC$_4$H$_8$)$_3$ ligand.

Comparison between the Cp- and Cp*-based systems also affords a look into the effects of electronic properties of the ancillary ligand as it contributes to the enthalpy of reaction. The Cp values are, on average, 4.4 kcal/mol more exothermic than the corresponding Cp* values. This was previously explained in terms of increased metal basicity in the Cp*-based system which corresponded to lower enthalpies of binding of a basic ligand. This difference in electronic properties at the metal center gauges a change in metal basicity. Sowa and Angelici have investigated a series of iridium complexes and have observed a difference in enthalpies of protonation of 5.7 kcal/mol between CpIr(COD) and Cp*Ir(COD) complexes.[24] In these experiments, H$^+$ proved to be more strongly bound to M−Cp* by ca. 5 kcal/mol. This is in view of the increased electron density imparted by the better Cp* donor. Wang and Angelici have also performed a similar analysis for the Cp′Ir(CO)(PR$_3$) system with similar results.[25] Hoff and co-workers have demonstrated this difference in metal basicity between Cp and Cp* in their thermochemical investigations of organomolybdenum complexes.[17a] In comparison of the enthalpy values for the tris(amino)phosphine series in the two systems, a similar ranking is observed, with some minor exchange of position. This may be due to the difference in the electronic picture at the metal on going from Cp to Cp* but also may include a constant steric component since the Cp* is more sterically demanding than its unmethylated congener.

Structural Studies of Cp*Ru[P(NR$_2$)$_{3-x}$(C$_6$H$_5$)$_x$]$_2$Cl Complexes (x = 0−2). In an effort to structurally compare the members of the series, single crystals of five complexes bearing the Cp*Ru(P(NR$_2$)$_3$)$_2$Cl composition were examined by X-ray diffraction techniques. This represents the first comprehensive structural study of metal complexes bearing the entire P(NR$_2$)$_3$ series. Salient structural features of the five related organoruthenium complexes examined are presented in Table 10.

General trends are worth mentioning. On going to greater phenyl-substituted phosphines (in the pyrolyl series), the Cp*(centroid)−Ru distance decreases, the Ru−Cl distance increases, and the average Ru−P distance increases. Such a significant overall variation of bond distances is not observed in related ruthenium phosphine complexes where σ donation dominates the bonding picture.[7i] There exists, in these systems, significant π contributions to the bonding which could

---

[21] Thermochemical investigation of this ligand series to the Fe(CO)$_3$ moiety afforded unprecedented isolation of the axial/equatorial isomer in addition to the thermodynamically more stable diaxial isomer. This is attributed to the efficient π back-donation into the pyrrolyl portion of the phosphine ligands: Serron, S. A.; Nolan, S. P. *Inorg. Chim. Acta* **1996**, *250*, in press. Examples of axial/equatorial substitutions in (PR$_3$)Fe(CO)$_4$ systems can be found in: Howell, J. A. S.; Palin, M. G.; McArdle, P.; Cunningham, D.; Goldschmidt, Z.; Gottlieb, H. E.; Hezroni-Langerman, D. *Inorg. Chem.* **1993**, *32*, 3493−3500.

[22] Serron, S. A.; Nolan, S. P. *Organometallics*, submitted for publication.

[23] It should be stated that a single electronic parameter to the enthalpy of reaction fit does not lead to a good or even a fair correlation (R = 0.54)

[24] a) Sowa, J. R., Jr.; Angelici, R. J. *J. Am. Chem. Soc.* **1991**, *113*, 2537−2544. (b) Rottink, M. K.; Angelici, R. J. *J. Am. Chem. Soc.* **1993**, *115*, 7267−7274.

[25] Wang, D.; Angelici, R. J. *Inorg. Chem.* **1996**, *35*, 1321−1331.

Table 10. Important Structural Parameters for $(C_5Me_5)Ru(P(NR_2)_3)_2Cl$ Complexes

complex	Cp(c)−Ru, Å	Ru−P, Å	Ru−Cl, Å	Cp(c)−Ru−L, deg	P−Ru−P, deg
$Cp^*Ru[P(NC_4H_4)_3]_2Cl$ (**2**)	1.930	2.2598(11)	2.4312(12)	114.8, Cl	95.83(4)
		2.2639(12)		127.0, P(1)	
				126.3, P(2)	
$Cp^*Ru[P(NC_4H_4)_2(C_6H_5)]_2Cl$ (**3**)	1.911	2.2871(14)	2.4373(14)	117.0, Cl	95.54(5)
		2.2827(14)		124.8, P(1)	
				127.3, P(2)	
$Cp^*Ru[P(NC_4H_4)(C_6H_5)_2]_2Cl$ (**4**)	1.900	2.3064(13)	2.443(2)	118.5, Cl	97.87(5)
		2.3195(14)		126.5, P(1)	
				125.3, P(2)	
$Cp^*Ru[P(NC_4H_8)_3]_2Cl$ (**5**)	1.943	2.3477(14)	2.4534(14)	113.7, Cl	97.59(4)
		2.3520 (14)		126.5, P(1)	
				125.9, P(2)	
$Cp^*Ru[P(NC_4H_8)_2Cl]_2Cl$ (**6**)	1.905	2.275(2)	2.433(2)	118.0, Cl	95.63(6)
		2.265(2)		128.5, P(1)	
				124.6, P(2)	

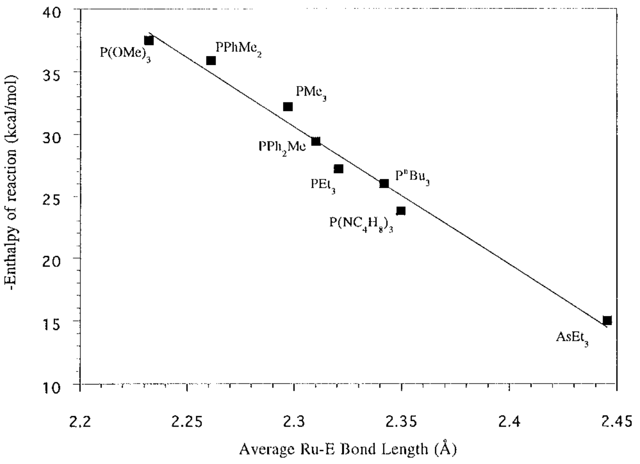

Figure 8. Enthalpy of ligand substitution reaction vs average Ru−E bond distance in the $Cp^*Ru(PR_3)_2Cl$ complexes. Slope = −110.9; $R = 0.99$.

facilitate electronic communication between molecular components. Another important structural feature is the observed increase in P−N bond distance on going from the $P(NC_4H_4)_3$ to the $P(NC_4H_4)_2(C_6H_5)$ to the $P(NC_4H_4)(C_6H_5)_2$ complex: gradually increasing from 1.720(4) to 1.733(5) to 1.750 (5) Å indicating that as a better donor is present this electron density is channeled through the pyrrolyl π system. The $P(NC_4H_8)_2Cl$ ligand and complex were synthesized to examine the feasibility and synthetic access to these complexes in order to gauge the effect of a Cl substituent. The complex behaves like $Cp^*Ru(P(NC_4H_4)_2(C_6H_5))_2Cl$. The chloride substituent is suspected to participate in π bonding in the present system. As for the pyrrolidinyl-substituted phosphine, $P(NC_4H_8)_3$, it structurally behaves very much like a σ donor, without significant π character. To test this observation, a simple bond length/bond strength relationship was established (Figure 8). The $P(NC_4H_8)_3$ complex behaves like other alkyl-substituted tertiary phosphines.

It should be mentioned here that the pyrrolyl-substituted phosphine complexes significantly deviate from the linear relationship illustrated in Figure 8. It appears that any π character to the ligand will cause serious deviations from this relationship. One point of interest in this system is the good fit displayed by the $P(OMe)_3$ complex,[26] although π involvement might be suspected for a phosphite ligand, it does not appear to be significant in the present system.

Moloy and Petersen have reported structural features of the $P(NC_4H_4)_3$ and $P(NC_4H_8)_3$ bound to the ClRh(CO) moiety.[13] Results within the ruthenium-based series enable comparisons between the two systems. Similar structural trends are observed for the M−P and M−Cl bond distances. Bonding of the $P(NC_4H_4)_3$ ligand leads to shorter metal−Cl and metal−phosphine distances compared to the $P(NC_4H_8)_3$ relative and is indicative of significant π bonding in the pyrrolyl-substituted phosphine ligands. In the rhodium system, the presence of the CO ligand permits a quantitative treatment (by infrared) of the π back-donation involved in this system and allows a qualitative binding affinity scale to be established. Pyramidization of one of the nitrogen atoms on a pyrrolidinyl ring is a similar feature displayed by the ruthenium and rhodium systems. The structure of complex **5** reveals the presence of a pyramidal nitrogen N(4) which exhibits a longer N−P bond length (1.710(4) Å) than those involving the planar nitrogens (average 1.694(4) Å). This difference in N−P bond length of 0.02 Å between planar and pyramidal nitrogen is also found to exist in the rhodium system studied by Moloy.[13] This appears to be a general feature since other examples of this pyramidization effect are found in the literature.[27,28] Further thermochemical studies are in progress in order to examine the binding ability of these novel ligands to other metal centers.

Conclusion

The labile nature of the COD ligand in CpRu(COD)Cl and Cp*Ru(COD)Cl was used to gain access into the thermochemistry of ligand substitution for N-substituted tertiary phosphine ligands. The enthalpy trend can

---

[26] Nolan, S. P.; Fagan, P. J.; Luo, L.; Li, C.; Stevens, E. D.; Jones, N. L. Manuscript in preparation.

[27] For a discussion of the electronic structure of tris(dialkylamino)phosphines see the following and references therein: (a) Cowey, A. H.; Lattman, M.; Stricklen, P. M.; Verkade, J. G. *Inorg. Chem.* **1982**, *21*, 543−549. (b)Hargis, J. H.; Worley, S. D. *Inorg. Chem.* **1977**, *16*, 1686- 1689.

[28] For X-ray crystallographic characterization of this effect see: (a) Xi, S. K.; Schmidt, H.; Lensink, C.; Kim, S.; Winmtergrass, D.; Daniels, L. M.; Jacobson, R. A.; Verkade, J. G. *Inorg. Chem.* **1990**, *29*, 2214−2220. (b) Hunt, J. J.; Duesler, E. N.; Paine, R. T. *J. Organomet. Chem.* **1987**, *320*, 307−315. (c) Socol, S. M.; Jacobson, R. A.; Verkade, J. G. *Inorg. Chem.* **1984**, *23*, 88−94. (d) Cowley, A. H.; Davis, R. E.; Remadna, K. *Inorg. Chem.* **1981**, *20*, 2146−2152.

be explained in terms of overwhelming steric contribution to the enthalpy of reaction. The increased exothermicity displayed by the CpRu(PR$_3$)$_2$Cl system over its Cp* parent is taken as a gauge of the increased metal basicity on going from Cp to Cp*. A quantitative relationship is established between structural and thermodynamic parameters and displays a good correlation for complexes having σ bonding as principal bonding component. Structural studies have been performed on five members of this ruthenium−*N*-phosphine series, and principal features deal with π involvement in the bonding of these complexes which make them weak binding ligands in the present systems. Further thermochemical, kinetic, mechanistic, and catalytic investigations focusing on this and related systems are presently underway.

Acknowledgment. The Board of Regents of the Louisiana Education Quality Support Fund (LEQSF-(RF/1993-96)-RD-A-47), the National Science Foundation (CHE-9631611 to S.P.N.), and DuPont (Educational Aid Grant) are gratefully acknowledged for support of this research. J.L.P. acknowledges financial support by the Chemical Instrumentation Program of the National Science Foundation (CHE-9120098) for the acquisition of the X-ray diffractometer. We are indebted to Aesar/Johnson-Matthey for the generous loan of ruthenium salts. We are also thankful to Dr. Kenneth Moloy (DuPont) for helpful discussions.

Supporting Information Available: Tables of atomic coordinates and *U* values, selected distances and angles, anisotropic thermal displacement parameters, and hydrogen bond distances for **2**−**6** (30 pages). Ordering information is given on any current masthead page.

OM960265F